Alexandria Engineering Journal (2023) 67, 643–653

HOSTED BY

ELSEVIER

Alexandria University

Alexandria Engineering Journal

www.elsevier.com/locate/aej
www.sciencedirect.com

ORIGINAL ARTICLE

A computational approach based on the fractional Euler functions and Chebyshev cardinal functions for distributed-order time fractional 2D diffusion equation

M.H. Heydari [a,*], M. Hosseininia [a], D. Baleanu [b,c,d]

[a] *Department of Mathematics, Shiraz University of Technology, Shiraz, Iran*
[b] *Department of Mathematics, Cankaya University, Ankara, Turkey*
[c] *Institute of Space Sciences, Magurele-Bucharest R76900, Romania*
[d] *Lebanese American University, Beirut, Lebanon*

Received 10 November 2022; revised 17 December 2022; accepted 30 December 2022
Available online 10 January 2023

KEYWORDS

Fractional Euler functions;
Chebyshev cardinal functions;
Distributed-order fractional derivative;
Diffusion equation

Abstract In this paper, the distributed-order time fractional diffusion equation is introduced and studied. The Caputo fractional derivative is utilized to define this distributed-order fractional derivative. A hybrid approach based on the fractional Euler functions and 2D Chebyshev cardinal functions is proposed to derive a numerical solution for the problem under consideration. It should be noted that the Chebyshev cardinal functions process many useful properties, such as orthogonality, cardinality and spectral accuracy. To construct the hybrid method, fractional derivative operational matrix of the fractional Euler functions and partial derivatives operational matrices of the 2D Chebyshev cardinal functions are obtained. Using the obtained operational matrices and the Gauss–Legendre quadrature formula as well as the collocation approach, an algebraic system of equations is derived instead of the main problem that can be solved easily. The accuracy of the approach is tested numerically by solving three examples. The reported results confirm that the established hybrid scheme is highly accurate in providing acceptable results.

1. Introduction

Due to the importance of fractional partial differential equations in modeling various problems in mathematics, physics, and engineering, many studies have been done on such problems. For instance, see [1–12]. Researchers have utilized numerical approaches instead of analytical ones to solve these

* Corresponding author.
E-mail addresses: heydari@sutech.ac.ir (M.H. Heydari), m.hosseininia@sutech.ac.ir (M. Hosseininia), dumitru@cankaya.edu.tr (D. Baleanu).

Peer review under responsibility of Faculty of Engineering, Alexandria University.

https://doi.org/10.1016/j.aej.2022.12.065
1110-0168

equations because it is difficult or impossible to achieve their true solution. Some of these schemes include meshless method [13], wavelet approach [14], piecewise spectral-collocation technique [15] and Touchard wavelet scheme [16]. The distributed-order (DO) fractional derivatives are a generalization of the classical fractional derivatives. These derivatives are derived by the classical integration upon the order of fractional derivative within a given domain [17]. DO fractional differential equations can be considered as a generalization of ordinary fractional differential equations. Such differential equations have been appeared in modeling of diverse problems in the fields of diffusion [18], viscoelastic [19], electronic oscillator [20], control [21], etc. Recently, much attention has been paid to numerical approaches to solve these types of equations. Some of these methods are Müntz–Legendre polynomials method [22], fractional-order Bernoulli-Legendre functions approach [23], fractional-order generalized Taylor wavelets scheme [17], Galerkin finite element method [24], Legendre–Gauss collocation approach [25], and Legendre wavelets scheme [26]. The fractional diffusion equation is a famous equation in science and engineering that is a generalization of the classical diffusion equation. The fractional equation has been used in the diverse fields, such as viscoelastic materials [27], biology [28], chaotic dynamics of classical conservative systems [29], etc. In recent years, researchers have investigated the solution of classical fractional model of the diffusion equation by different numerical techniques. Some of methods used are meshless method [13], fractional reduced differential transform approach [30], Crank–Nicholson scheme [31], second-order ADI difference technique [32], exponential-sum-approximation method [33], etc. Nowadays, researchers prefer fractional basis functions to classical polynomials to construct numerical methods for solving fractional differential equations, because in dealing with fractional differential equations, there are usually a number of terms with fractional powers that are not compatible with classical polynomials. In fact, this drawback causes that the accuracy of methods generated using polynomials for such problems significantly reduces. To resolve this drawback, fractional functions are widely applied in recent years. In [34], Hosseininia et al. have applied a hybrid method based on the Müntz-Legender functions and 2D Müntz-legender wavelets for solving fractional Sobolev equation. The authors of [35] have used fractional order Legendre wavelets for the numerical solution of pantograph differential equation. A computational approach using fractional-order Legendre functions have been utilized in [36] to solve fractional convective straight fin model. The authors of [37] proposed an accurate technique based on the fractional alternative Legendre functions to solve on linear fractional integro-differential equation. In this paper, we employ fractional Euler functions (FEFs) (that are constructed using Euler polynomials) to create a numerical method for the above stated problem. We remind that during last years, these functions have been effectively employed to solve various problems, such as fractional-order delay integro-differential equations [38], fractional partial differential equations [39], fractional integro-differential equations [40], fractional diffusion equations [41], etc. The Chebyshev cardinal functions (CCFs) as a well-known family of cardinal functions have been widely applied for solving divers problems in recent years. Some of problems solved with the aid of these polynomials include fractional fourth-order 2D Kuramoto–Sivashinsky problem [42], coupled nonlinear fractal-fractional Schrödinger equations [43], telegraph equation [45], nonlinear optimal control problems [46], partial differential equation [47], Sturm–Liouville problem [48], etc. Note that these functions have several useful properties, such as cardinality and exponential accuracy [43]. The main objectives of this article are briefly given in the follows:

- Introducing the FEFs and obtaining their fractional derivative matrix.
- Investigating the CCFs for two-dimensional problems and obtaining their derivative matrices.
- Introducing a new form of the fractional 2D diffusion equation with DO fractional derivative.
- Proposing a hybrid method based on the FEFs and 2D CCFs for the numerical solution of such problems.

So, we focus on the DO fractional diffusion problem

$$\int_0^1 \varpi(\mu)\,{}_0^C D_t^{\mu} \upsilon(x,y,t)\,d\mu = \alpha\Delta\upsilon(x,y,t) + F(x,y,t),$$
$$(x,y)\in\Omega=[0,1]^2,\ \ t\in[0,1], \tag{1.1}$$

with the initial condition

$$\upsilon(x,y,0)=v(x,y),\ \ (x,y)\in\Omega, \tag{1.2}$$

and boundary conditions

$$\begin{aligned} &\upsilon(0,y,t)=\xi_1(y,t), && \upsilon(1,y,t)=\xi_2(y,t),\\ &\upsilon(x,0,t)=\xi_3(x,t), && \upsilon(x,1,t)=\xi_4(x,t), \end{aligned} \tag{1.3}$$

where α is a real number, $F, v$and $\xi_\iota,\ \iota=1,2,3,4$ are given functions, and the function υ is the undetermined solution of the problem. Moreover, ${}_0^C D_t^{\mu}$ expresses the Caputo fractional derivative of order μ, which will be provided in the next section. Also, the distribution function $\varpi:[0,1]\to\mathbb{R}^+\cup\{0\}$satisfies the following conditions [44]:

$$\forall\mu\in[0,1],\ \ \varpi(\mu)>0 \text{ and } 0<\int_0^1\varpi(\mu)\,d\mu<\infty. \tag{1.4}$$

To solve the DO problem introduced in (1.1), we propose a hybrid approach based on the FEFs and 2D CCFs. We first expand the problem solution in terms of the FEFs (in the temporal domain) and 2D CCFs (in the spatial domain) together. By calculating the fractional derivative of the FEFs, employing the Gauss-Legender quadrature formula, partial derivatives operational matrices of the 2D CCFs and the collocation technique, we convert solving this problem into solving an algebraic system. Some of the most important advantages of the suggested hybrid approach are listed in the following:

- Fractional-order basis functions can well invert the properties of fractional-order differential equations.
- Fractional-order functions have two degrees of freedom but polynomials have one degree of freedom.
- The CCFs process many useful properties such as orthogonality, cardinality, and spectral accuracy.
- A small value of basis functions is needed to achieve high accuracy and satisfactory results.
- By applying this method, the consideration problem is transformed into a system of algebraic equations that can be solved via a suitable numerical approach.

The rest of this article includes these sections: Required preparations are given in Section 2. The FEFs and their fractional derivative matrix are provided in Section 3. The CCFs and their partial derivatives matrices are investigated in Section 4. The hybrid technique is explained in Section 5. Three examples are given in Section 6. The conclusion of this study is provided in Section 7.

2. Preparations

In this section, the information required for the next sections is reviewed.

Definition 1. ([49]) The Caputo fractional derivative of order $0<\mu\leqslant 1$of the function $\hbar$(which is differentiable on its domain) is defined by

$$ {}_0^C D_t^{\mu}\hbar(t)=\begin{cases}\frac{1}{\Gamma(1-\mu)}\int_0^t (t-\bar{z})^{-\mu}\hbar'(\bar{z})\,d\bar{z}, & 0<\mu<1,\\ \hbar'(t), & \mu=1.\end{cases} \tag{2.1}$$

Corollary 1. ([49]) For $\mu\in(0,1)$ and $\varepsilon\in\mathbb{R}^+\cup\{0\}$, we have

$$ {}_0^C D_t^{\mu}t^{\varepsilon}=\begin{cases}0, & \varepsilon=0,\\ \frac{\Gamma(\varepsilon+1)}{\Gamma(\varepsilon-\mu+1)}\,t^{\varepsilon-\mu}, & \varepsilon\in\mathbb{R}^+.\end{cases} \tag{2.2}$$

Definition 2. ([50]) The Bernoulli polynomials of order $\kappa$are defined as

$$B_\kappa(t)=\sum_{l=0}^{\kappa}\binom{\kappa+1}{l}\varrho_l\,t^{\kappa-l},\ \kappa=0,1,\ldots, \tag{2.3}$$

in which $\varrho_l=B_l(0)$, $l=0,1,\ldots,\kappa$are the Bernoulli numbers.

3. The fractional Euler functions

In this section, we review the FEFs and investigate the approximation of a specific function by them and also compute their fractional derivative.

Definition 3. ([38]) The FEFs of order $\bar{\imath}$are defined upon $[0,1]$as

$$E_{\bar{\imath}}^{\beta}(t)=\frac{1}{\bar{\imath}+1}\sum_{r=1}^{\bar{\imath}+1}\left(2-2^{r+1}\right)\binom{i+1}{r}B_r(0)\,t^{\beta(\bar{\imath}-r+1)},\quad \bar{\imath}=0,1,\ldots, \tag{3.1}$$

where $B_r(0)$'s are the Bernoulli polynomials defined in (2.3).

Property 1. The following relation is satisfied for the FEFs:

$$\int_0^1 E_{\bar{\imath}}^{\beta}(t)E_{\bar{\jmath}}^{\beta}(t)t^{\beta-1}\,dt=(-1)^{\bar{\imath}-1}\frac{\bar{\jmath}!(\bar{\imath}+1)!}{\beta(\bar{\jmath}+\bar{\imath}+1)!}E_{\bar{\jmath}+\bar{\imath}+1}(0),\quad \bar{\imath},\bar{\jmath}\geqslant 0. \tag{3.2}$$

Applying the FEFs, we can expand a function $\vartheta\in L^2([0,1])$as follows:

$$\vartheta(t)\simeq\sum_{\bar{\imath}=0}^{\bar{n}}\gamma_{\bar{\imath}}E_{\bar{\imath}}^{\beta}(t)\triangleq\Gamma^T\mathbb{E}_{\bar{n}}^{\beta}(t), \tag{3.3}$$

where

$$\Gamma=[\gamma_0\,\gamma_1\,\ldots\,\gamma_{\bar{n}}]^T,$$

with

$$\gamma_{\bar{\imath}}=\int_0^1\vartheta(t)E_{\bar{\imath}}^{\beta}(t)t^{1-\beta}\,dt,$$

and

$$\mathbb{E}_{\bar{n}}^{\beta}(t)=\left[E_0^{\beta}(t)\,E_1^{\beta}(t)\,\ldots\,E_{\bar{n}}^{\beta}(t)\right]^T. \tag{3.4}$$

Theorem 1. The Caputo fractional derivative of order $0<\mu\leqslant 1$of the vector $\mathbb{E}_{\bar{n}}^{\beta}(t)$expressed in (3.4) can be computed as follows:

$${}_0^C D_t^{\mu}\mathbb{E}_{\bar{n}}^{\beta}(t)=\mathbf{D}_t^{(\mu,\beta)}(t)\,\mathbb{E}_{\bar{n}}^{\beta}(t), \tag{3.5}$$

where $\mathbf{D}_t^{(\mu,\beta)}(t)$ is an $(\bar{n}+1)\times(\bar{n}+1)$matrix as

$$\mathbf{D}_t^{(\mu,\beta)}(t)=\Theta\mathbb{D}_t^{(\mu,\beta)}(t)(\Theta)^{-1},$$

with

$$[\Theta]_{\bar{k}\bar{\ell}}=\begin{cases}0, & \bar{k}<\bar{\ell},\\ \frac{2-2^{\bar{k}-\bar{\ell}+2}}{k}\binom{\bar{k}}{\bar{k}-\bar{\ell}+1}B_{\bar{k}-\bar{\ell}+2}(0), & \bar{k}\geqslant\bar{\ell},\end{cases}$$

for $\bar{k},\bar{\ell}=1,2,\ldots,\bar{n}+1$, and

$$\mathbb{D}_t^{(\mu,\beta)}(t)=t^{-\mu}\mathrm{diag}\left(0,\frac{\Gamma(\beta+1)}{\Gamma(\beta-\mu+1)},\ldots,\frac{\Gamma(\bar{n}\beta+1)}{\Gamma(\bar{n}\beta-\mu+1)}\right),$$

in which diag means diagonal matrix.

Proof. The vector $\mathbb{E}_{\bar{n}}^{\beta}(t)$ in (3.4) can be rewritten as

$$\mathbb{E}_{\bar{n}}^{\beta}(t)=\begin{pmatrix}E_0^{\beta}(t)\\E_1^{\beta}(t)\\ \vdots\\ E_{\bar{n}}^{\beta}(t)\end{pmatrix}=\underbrace{\begin{pmatrix}\frac{2-2^2}{1}\binom{1}{1}B_1(0) & 0 & \ldots & 0\\ \frac{2-2^3}{2}\binom{2}{2}B_2(0) & \frac{2-2^2}{2}\binom{2}{1}B_1(0) & \ldots & 0\\ \vdots & \vdots & \ddots & \vdots\\ \frac{2-2^{\bar{n}+2}}{\bar{n}+1}\binom{\bar{n}+1}{\bar{n}+1}B_{\bar{n}+1}(0) & \frac{2-2^{\bar{n}+1}}{\bar{n}+1}\binom{\bar{n}+1}{\bar{n}}B_{\bar{n}}(0) & \ldots & \frac{2-2^2}{\bar{n}+1}\binom{\bar{n}+1}{1}B_1(0)\end{pmatrix}}_{\Theta}\times\underbrace{\begin{pmatrix}1\\t^{\beta}\\ \vdots\\ t^{\bar{n}\beta}\end{pmatrix}}_{T^{\beta}(t)}=\Theta T^{\beta}(t). \tag{3.6}$$

So, we have

$${}_0^C D_t^{\mu}\mathbb{E}_{\bar{n}}^{\beta}(t)={}_0^C D_t^{\mu}\Theta T^{\beta}(t)=\Theta{}_0^C D_t^{\mu}T^{\beta}(t). \tag{3.7}$$

On the other hand, we have

$${}_0^C D_t^{\mu}T^{\beta}(t)=t^{-\mu}\underbrace{\begin{pmatrix}0 & 0 & \ldots & 0\\ 0 & \frac{\Gamma(\beta+1)}{\Gamma(\beta-\mu+1)} & \ldots & 0\\ \vdots & \vdots & \ddots & \vdots\\ 0 & 0 & \ldots & \frac{\Gamma(\bar{n}\beta+1)}{\Gamma(\bar{n}\beta-\mu+1)}\end{pmatrix}}_{\mathbb{D}_t^{(\mu,\beta)}(t)}\begin{pmatrix}1\\t^{\beta}\\ \vdots\\ t^{\bar{n}\beta}\end{pmatrix}=\mathbb{D}_t^{(\mu,\beta)}(t)\,T^{\beta}(t). \tag{3.8}$$

From (3.6) and (3.8), we get

$${}_0^C D_t^{\mu}\mathbb{E}_{\bar{n}}^{\beta}(t)=\Theta\mathbb{D}_t^{(\mu,\beta)}(t)\,T^{\beta}(t)=\Theta\mathbb{D}_t^{(\mu,\beta)}(t)(\Theta)^{-1}\mathbb{E}_{\bar{n}}^{\beta}(t),$$

which ended the proof.

4. The Chebyshev cardinal functions

In this section, the 1D and 2D CCFs with their property are briefly presented.

4.1. The 1D Chebyshev cardinal functions

A set with $(\bar{m}_1+1)$ elements of the 1D CCFs can be generated on the interval $[0, x_{max}]$as follows [43]:

$$\phi_{\bar{i}}(x) = \prod_{\bar{k}=1,\bar{k}\neq\bar{i}}^{\bar{m}_1+1} \frac{x - x_{\bar{k}}}{x_{\bar{i}} - x_{\bar{k}}}, \quad \bar{i} = 1, 2, \ldots, \bar{m}_1 + 1, \tag{4.1}$$

where $x_{\bar{k}} = \frac{x_{max}}{2}\left[1 - \cos\left(\frac{(2\bar{k}-1)\pi}{2(\bar{m}_1+1)}\right)\right]$and $x_{\bar{k}}$'s are the shifted zeros of the $(\bar{m}_1+1)$th Chebyshev polynomial over $[-1, 1]$[51].

Remark 1. ([43]) The 1D CCFs demonstrated in (4.1) can also be defined as follows:

$$\phi_{\bar{i}}(x) = \frac{1}{\bar{\gamma}_{\bar{i}}} \sum_{\bar{k}=0}^{\bar{m}} \bar{b}_{\bar{i}\bar{k}} x^{\bar{m}-\bar{k}}, \quad \bar{i} = 1, 2, \ldots, \bar{m} + 1, \tag{4.2}$$

where

$$\bar{\gamma}_{\bar{i}} = \prod_{\bar{\ell}=1,\bar{\ell}\neq\bar{i}}^{\bar{m}_1+1} (x_{\bar{i}} - x_{\bar{\ell}}),$$

and

$$\bar{b}_{\bar{i}\bar{k}} = \begin{cases} 1, & \bar{k} = 0, \\ \frac{-1}{\bar{k}} \sum_{\bar{\ell}=1}^{\bar{k}} \bar{a}_{\bar{i}\bar{\ell}} \bar{b}_{\bar{i}\,\bar{k}-\bar{\ell}}, & \bar{k} = 1, 2, \ldots, \bar{m}, \end{cases}$$

in which

$$\bar{a}_{\bar{i}\bar{\ell}} = \sum_{\bar{r}=1,\bar{r}\neq\bar{i}}^{\bar{m}+1} x_{\bar{r}}^{\bar{\ell}}, \quad 1 \leqslant \bar{\ell} \leqslant \bar{k}.$$

4.2. The 2D Chebyshev cardinal functions

By employing the CCFs in the one dimension, we can make the 2D CCFs on the domain $[0, x_{max}] \times [0, y_{max}]$as follows:

$$\psi_{\iota\varsigma}(x, y) = \phi_\iota(x)\phi_\varsigma(y), \quad 1 \leqslant \iota \leqslant \bar{m}_1 + 1, \ 1 \leqslant \varsigma \leqslant \bar{m}_2 + 1. \tag{4.3}$$

We can approximate any two-variables function $\rho \in C([0, x_{max}] \times [0, y_{max}])$by the 2D CCFs as follows:

$$\rho(x, y) \simeq \sum_{\iota=1}^{\bar{m}_1+1} \sum_{\varsigma=1}^{\bar{m}_2+1} \rho_{\iota\varsigma} \psi_{\iota\varsigma}(x, y) \triangleq \mathbf{P}^T \Psi_{\bar{m}_1\bar{m}_2}(x, y), \tag{4.4}$$

where

$$\mathbf{P} = \left[\rho_{11}\ \rho_{12}\ \ldots\ \rho_{1(\bar{m}_2+1)} | \ldots | \rho_{(\bar{m}_1+1)1}\ \rho_{(\bar{m}_1+1)2}\ \ldots\ \rho_{(\bar{m}_1+1)(\bar{m}_2+1)}\right]^T,$$

with

$$\rho_{\iota\varsigma} = \rho(x_\iota, y_\varsigma), \quad \iota = 1, 2, \ldots, \bar{m}_1 + 1, \ \varsigma = 1, 2, \ldots, \bar{m}_2 + 1,$$

and

$$\Psi_{\bar{m}_1\bar{m}_2}(x, y) = \left[\psi_{11}(x, y)\ \psi_{12}(x, y)\ \ldots\ \psi_{1(\bar{m}_2+1)}(x, y) | \ldots | \psi_{(\bar{m}_1+1)1}(x, y)\ \psi_{(\bar{m}_1+1)2}(x, y)\ \ldots\ \psi_{(\bar{m}_1+1)(\bar{m}_2+1)}(x, y)\right]^T. \tag{4.5}$$

Theorem 2. The second-order partial derivative of the vector $\Psi_{\bar{m}_1\bar{m}_2}(x, y)$expressed in (4.5) with respect to x can be expressed in the form of

$$\frac{\partial^2 \Psi_{\bar{m}_1\bar{m}_2}(x, y)}{\partial x^2} = \mathrm{D}_x^{(2)} \Psi_{\bar{m}_1\bar{m}_2}(x, y), \tag{4.6}$$

where $\mathrm{D}_x^{(2)}$is an $(\bar{m}_1+1)(\bar{m}_2+1) \times (\bar{m}_1+1)(\bar{m}_2+1)$matrix as

$$\mathrm{D}_x^{(2)} = \begin{pmatrix} \bar{d}_{11}^{(2)}\mathscr{I} & \bar{d}_{12}^{(2)}\mathscr{I} & \ldots & \bar{d}_{1(\bar{m}_1+1)}^{(2)}\mathscr{I} \\ \bar{d}_{21}^{(2)}\mathscr{I} & \bar{d}_{22}^{(2)}\mathscr{I} & \ldots & \bar{d}_{2(\bar{m}_1+1)}^{(2)}\mathscr{I} \\ \vdots & \vdots & \ddots & \vdots \\ \bar{d}_{(\bar{m}_1+1)1}^{(2)}\mathscr{I} & \bar{d}_{(\bar{m}_1+1)2}^{(2)}\mathscr{I} & \ldots & \bar{d}_{(\bar{m}_1+1)(\bar{m}_1+1)}^{(2)}\mathscr{I} \end{pmatrix},$$

with

$$\bar{d}_{\bar{i}\bar{j}}^{(2)} = \frac{1}{\bar{\gamma}_{\bar{i}}} \sum_{\bar{\ell}=0}^{\bar{m}_1-2} \bar{b}_{\bar{i}\bar{\ell}} (\bar{m}_1 - \bar{\ell})(\bar{m}_1 - \bar{\ell} - 1) x_{\bar{j}}^{\bar{m}_1-\bar{\ell}-2}, \quad \bar{i}, \bar{j} = 1, 2, \ldots, \bar{m}_1 + 1,$$

and

$$[\mathscr{I}]_{\bar{i}\bar{j}} = \begin{cases} 1, & \bar{i} = \bar{j}, \ \bar{i}, \bar{j} = 1, 2, \ldots, \bar{m}_2 + 1, \\ 0, & \text{otherwise}. \end{cases}$$

Proof. The proof is easy. So, we leave it to interested reader.

Theorem 3. We can express the second-order partial derivative of the vector $\Psi_{\bar{m}_1\bar{m}_2}(x, y)$given in (4.5), with respect to y in the form of

$$\frac{\partial^2 \Psi_{\bar{m}_1\bar{m}_2}(x, y)}{\partial y^2} = \mathrm{D}_y^{(2)} \Psi_{\bar{m}_1\bar{m}_2}(x, y), \tag{4.7}$$

where $\mathrm{D}_y^{(2)}$is $(\bar{m}_1+1)(\bar{m}_2+1) \times (\bar{m}_1+1)(\bar{m}_2+1)$matrix as

$$\mathrm{D}_y^{(2)} = \begin{pmatrix} \mathscr{D}^{(2)} & \overline{O} & \ldots & \overline{O} \\ \overline{O} & \mathscr{D}^{(2)} & \ldots & \overline{O} \\ \vdots & \vdots & \ddots & \vdots \\ \overline{O} & \overline{O} & \ldots & \mathscr{D}^{(2)} \end{pmatrix},$$

in which $\overline{O}$ is an $(\bar{m}_2+1) \times (\bar{m}_2+1)$zero matrix and

$$\left[\mathscr{D}^{(2)}\right]_{\bar{i}\bar{j}} = \frac{1}{\bar{\gamma}_{\bar{i}}} \sum_{\bar{\ell}=0}^{\bar{m}_2-2} \bar{b}_{\bar{i}\bar{\ell}} (\bar{m}_2 - \bar{\ell})(\bar{m}_2 - \bar{\ell} - 1) y_{\bar{j}}^{\bar{m}_2-\bar{\ell}-2},$$

$\bar{i}, \bar{j} = 1, 2, \ldots, \bar{m}_2 + 1,$

where $y_{\bar{j}} = \frac{y_{max}}{2}\left[1 - \cos\left(\frac{(2\bar{j}-1)\pi}{2(\bar{m}_2+1)}\right)\right]$and $y_{\bar{j}}$'s are the shifted zeros of the $(\bar{m}_2+1)$th Chebyshev polynomial over $[-1, 1]$.

Proof. The proof is straightforward. So, we leave it to interested reader.

As a numerical example, for $\bar{m}_1 = 2, \bar{m}_2 = 3$, we have

$$\mathrm{D}_y^{(2)} = \begin{pmatrix} 22.627 & 12.686 & -1.3726 & -11.314 & 0 & 0 & 0 & 0 & 0 & 0 & 0 & 0 \\ -46.627 & -22.627 & 11.314 & 35.314 & 0 & 0 & 0 & 0 & 0 & 0 & 0 & 0 \\ 35.314 & 11.314 & -22.627 & -46.627 & 0 & 0 & 0 & 0 & 0 & 0 & 0 & 0 \\ -11.314 & -1.3726 & 12.686 & 22.627 & 0 & 0 & 0 & 0 & 0 & 0 & 0 & 0 \\ 0 & 0 & 0 & 0 & 22.627 & 12.686 & -1.3726 & -11.314 & 0 & 0 & 0 & 0 \\ 0 & 0 & 0 & 0 & -46.627 & -22.627 & 11.314 & 35.314 & 0 & 0 & 0 & 0 \\ 0 & 0 & 0 & 0 & 35.314 & 11.314 & -22.627 & -46.627 & 0 & 0 & 0 & 0 \\ 0 & 0 & 0 & 0 & -11.314 & -1.3726 & 12.686 & 22.627 & 0 & 0 & 0 & 0 \\ 0 & 0 & 0 & 0 & 0 & 0 & 0 & 0 & 22.627 & 12.686 & -1.3726 & -11.314 \\ 0 & 0 & 0 & 0 & 0 & 0 & 0 & 0 & -46.627 & -22.627 & 11.314 & 35.314 \\ 0 & 0 & 0 & 0 & 0 & 0 & 0 & 0 & 35.314 & 11.314 & -22.627 & -46.627 \\ 0 & 0 & 0 & 0 & 0 & 0 & 0 & 0 & -11.314 & -1.3726 & 12.686 & 22.627 \end{pmatrix}.$$

5. The hybrid method

This section explains a hybrid method based on the FEFs and 2D CCFs for the introduced DO fractional problem in the first section of this paper.

From (3.3) and (4.4), we can consider the following approximation:

$$\upsilon(x,y,t) \simeq \Psi^T_{\bar{m}_1\bar{m}_2}(x,y)\Lambda\,\mathbb{E}^{\beta}_{\bar{n}}(t), \tag{5.1}$$

where Λ is an unknown $(\bar{m}_1+1)(\bar{m}_2+1)\times(\bar{n}+1)$matrix. We obtain the following relation by using (3.5) and (5.1):

$$\begin{aligned} \int_0^1 \varpi(\mu)\,{}_0^C D_t^{\mu}\upsilon(x,y,t)\,d\mu &\simeq \Psi^T_{\bar{m}_1\bar{m}_2}(x,y)\Lambda \int_0^1 \varpi(\mu)\mathbf{D}_t^{(\mu,\beta)}(t)\mathbb{E}^{\beta}_{\bar{n}}(t)\,d\mu \\ &\simeq \Psi^T_{\bar{m}_1\bar{m}_2}(x,y)\Lambda \int_0^1 \varpi(\mu)\Theta\mathbb{D}_t^{(\mu,\beta)}(t)(\Theta)^{-1}\mathbb{E}^{\beta}_{\bar{n}}(t)\,d\mu \\ &\simeq \Psi^T_{\bar{m}_1\bar{m}_2}(x,y)\Lambda \int_0^1 \varpi(\mu)\Theta t^{-\mu}\mathrm{diag}\left(0,\tfrac{\Gamma(\beta+1)}{\Gamma(\beta-\mu+1)},\ldots,\tfrac{\Gamma(\bar{n}\beta+1)}{\Gamma(\bar{n}\beta-\mu+1)}\right) \\ &\times(\Theta)^{-1}\left[\mathbb{E}^{\beta}_0(t)\;\mathbb{E}^{\beta}_1(t)\;\ldots\;\mathbb{E}^{\beta}_{\bar{n}}(t)\right]^T d\mu \\ &\simeq \Psi^T_{\bar{m}_1\bar{m}_2}(x,y)\Lambda \int_0^1 \varpi(\mu)\mathbb{D}^{(\beta)}(t,\mu)\,d\mu, \end{aligned} \tag{5.2}$$

where $\mathbb{D}^{(\beta)}(t,\mu) = \Theta t^{-\mu}\mathrm{diag}\left(0,\frac{\Gamma(\beta+1)}{\Gamma(\beta-\mu+1)},\ldots,\frac{\Gamma(\bar{n}\beta+1)}{\Gamma(\bar{n}\beta-\mu+1)}\right)(\Theta)^{-1}$ $\left[\mathbb{E}^{\beta}_0(t)\;\mathbb{E}^{\beta}_1(t)\;\ldots\;\mathbb{E}^{\beta}_{\bar{n}}(t)\right]^T$.

Using the Gauss–Legendre integration formula, we can calculate the integral in (5.2) as follows:

$$\begin{aligned} \int_0^1 \varpi(\mu)\mathbb{D}^{(\beta)}(t,\mu)\,d\mu &\simeq \frac{1}{2}\sum_{\iota=0}^{\bar{N}}\omega_\iota\varpi\left(\frac{1}{2}(\tau_\iota+1)\right)\mathbb{D}^{(\beta)}\left(t,\frac{1}{2}(\tau_\iota+1)\right) \\ &\simeq \mathbb{P}^{(\beta)}(t), \end{aligned} \tag{5.3}$$

where

$$\omega_\iota = \frac{2}{\left(1-\tau_\iota^2\right)\left(L'_{\bar{N}+1}(\tau_\iota)\right)^2},$$

and $\{\tau_\iota\}_{\iota=0}^{\bar{N}}$are zeros of $L_{\bar{N}+1}(\tau)$ in $[-1,1]$(for a given $\widehat{N}$). Substituting (5.3) into (5.2) yields

$$\int_0^1 \varpi(\mu)\,{}_0^C D_t^{\mu}\upsilon(x,y,t)\,d\mu \simeq \Psi^T_{\bar{m}_1\bar{m}_2}(x,y)\Lambda\,\mathbb{P}^{(\beta)}(t). \tag{5.4}$$

Utilizing (4.6) and (4.7), we get

$$\begin{aligned} \tfrac{\partial^2\Psi_{\bar{m}_1\bar{m}_2}(x,y)}{\partial x^2} &\simeq \Psi^T_{\bar{m}_1\bar{m}_2}(x,y)\left(\mathrm{D}_x^{(2)}\right)^T\Lambda\,\mathbb{E}^{\beta}_{\bar{n}}(t), \\ \tfrac{\partial^2\Psi_{\bar{m}_1\bar{m}_2}(x,y)}{\partial y^2} &\simeq \Psi^T_{\bar{m}_1\bar{m}_2}(x,y)\left(\mathrm{D}_y^{(2)}\right)^T\Lambda\,\mathbb{E}^{\beta}_{\bar{n}}(t). \end{aligned} \tag{5.5}$$

Substituting (5.1), (5.4) and (5.5) into (1.1), results in

$$\begin{aligned} \mathscr{R}(x,y,t) &\triangleq \Psi^T_{\bar{m}_1\bar{m}_2}(x,y)\Lambda\,\mathbb{P}^{(\beta)}(t) - \alpha\Psi^T_{\bar{m}_1\bar{m}_2}(x,y) \\ &\times\left[\left(\left(\mathrm{D}_x^{(2)}\right)^T + \left(\mathrm{D}_y^{(2)}\right)^T\right)\Lambda\right]\mathbb{E}^{\beta}_{\bar{n}}(t) - F(x,y,t) \simeq 0. \end{aligned} \tag{5.6}$$

The function $v(x,y)$in (1.2) can be expanded as

$$v(x,y) \simeq \Psi^T_{\bar{m}_1\bar{m}_2}(x,y)\,V, \tag{5.7}$$

where V is an $(\bar{m}_1+1)(\bar{m}_2+1)$ determined vector. According to (1.2), (5.1) and (5.7), we have

$$\upsilon(x,y,t) - v(x,y) \simeq \Psi^T_{\bar{m}_1\bar{m}_2}(x,y)\Big[\underbrace{\Lambda\mathbb{E}^{\beta}_{\bar{n}}(0) - V}_{V_1}\Big] \triangleq \mathbb{V}(x,y) \simeq 0. \tag{5.8}$$

The functions $\xi_\iota$for $\iota = 1,2,3,4$expressed in (1.3) can be approximated as

$$\xi_1(y,t) \simeq \Xi_1(y)\mathbb{E}^{\beta}(t), \quad \xi_2(y,t) \simeq \Xi_2(y)\mathbb{E}^{\beta}(t),$$
$$\xi_3(x,t) \simeq \Xi_3(x)\mathbb{E}^{\beta}(t), \quad \xi_4(x,t) \simeq \Xi_4(x)\mathbb{E}^{\beta}(t), \tag{5.9}$$

in which $\Xi_\imath$for $\imath = 1,2,3,4$are given vectors. From (1.3), (5.9) and (5.1), we get

$$\begin{aligned}
&\left[\Psi^T_{\bar{m}_1\bar{m}_2}(0,y)\Lambda - \Xi_1(y)\right]\mathbb{E}^{\beta}(t) \triangleq \bar{\Xi}_1(y,t) \simeq 0,\\
&\left[\Psi^T_{\bar{m}_1\bar{m}_2}(1,y)\Lambda - \Xi_2(y)\right]\mathbb{E}^{\beta}(t) \triangleq \bar{\Xi}_2(y,t) \simeq 0,\\
&\left[\Psi^T_{\bar{m}_1\bar{m}_2}(x,0)\Lambda - \Xi_3(x)\right]\mathbb{E}^{\beta}(t) \triangleq \bar{\Xi}_3(x,t) \simeq 0,\\
&\left[\Psi^T_{\bar{m}_1\bar{m}_2}(x,1)\Lambda - \Xi_4(x)\right]\mathbb{E}^{\beta}(t) \triangleq \bar{\Xi}_4(x,t) \simeq 0.
\end{aligned} \tag{5.10}$$

We derive an $(\bar{m}_1+1)(\bar{m}_2+1)\times(\bar{n}_1+1)$ system using (5.6), (5.8) and (5.10) as

$$\begin{cases}
\mathscr{R}(x_\imath, y_\jmath, t_\zeta) = 0, & \imath = 2,3,\ldots,\bar{m}_1,\ \jmath = 2,3,\ldots,\bar{m}_2,\ \zeta = 2,3,\ldots,\bar{n}+1,\\
\mathbb{V}(x_\imath, y_\jmath) = 0, & \imath = 1,2,\ldots,\bar{m}_1+1,\ \jmath = 1,2,\ldots,\bar{m}_2+1,\\
\bar{\Xi}_\eta(y_\jmath, t_\zeta) = 0, & \eta = 1,2,\ \jmath = 1,2,\ldots,\bar{m}_2+1,\ \zeta = 2,3,\ldots,\bar{n}+1,\\
\bar{\Xi}_\eta(x_\imath, t_\zeta) = 0, & \eta = 3,4,\ \imath = 2,\ldots,\bar{m}_1,\ \zeta = 2,3,\ldots,\bar{n}+1,
\end{cases} \tag{5.11}$$

with

$$x_\imath = \frac{1}{2}\left[1-\cos\left(\frac{(2\imath-1)\pi}{2(\bar{m}_1+1)}\right)\right],$$
$$y_\jmath = \frac{1}{2}\left[1-\cos\left(\frac{(2\jmath-1)\pi}{2(\bar{m}_2+1)}\right)\right],$$
$$t_\zeta = \frac{1}{2}\left[1-\cos\left(\frac{(2\zeta-1)\pi}{2(\bar{n}+1)}\right)\right].$$

Now, we can easily solve system (5.11) and find the vector Λ. Finally, we extract a solution for the DO fractional problem (1.1) by (5.1).

6. Results of numerical simulations

In the continuation, we have utilized the hybrid methodology explained in Section 5 for three examples. By helping these examples, we show the correctness of the explained approach. Assume that $\bar{\upsilon}(x,y,t)$is the approximation of $\upsilon(x,y,t)$, as the solution of the problem under study. We provide the following error formulae:

$$L_\infty = \max_{1\leqslant\imath\leqslant\bar{m}_1+1}\max_{1\leqslant\jmath\leqslant\bar{m}_2+1}\left|\upsilon(x_\imath,y_\jmath,1)-\bar{\upsilon}(x_\imath,y_\jmath,1)\right|,$$

$$L_2 = \left(\sum_{\imath=1}^{\bar{m}_1+1}\sum_{\jmath=1}^{\bar{m}_2+1}\left|\upsilon(x_\imath,y_\jmath,1)-\bar{\upsilon}(x_\imath,y_\jmath,1)\right|^2\right)^{1/2},$$

$$\mathrm{RMS} = \left(\frac{1}{(\bar{m}_1+1)(\bar{m}_2+1)}\left(\sum_{\imath=1}^{\bar{m}_1+1}\sum_{\jmath=1}^{\bar{m}_2+1}\left|\upsilon(x_\imath,y_\jmath,1)-\bar{\upsilon}(x_\imath,y_\jmath,1)\right|^2\right)\right)^{1/2}.$$

Moreover, we report the convergence order ($\mathscr{CO}$) of the provided scheme using the below formula:

$$\mathscr{CO} = \left|\frac{\log\left(\frac{L_\infty(\mathscr{M}_2)}{L_\infty(\mathscr{M}_1)}\right)}{\log\left(\frac{\mathscr{M}_2}{\mathscr{M}_1}\right)}\right|,$$

where $\mathscr{M}_1$and $\mathscr{M}_2$are the number of basic functions used in the first and second implantations, respectively. For numerical integration, we put $\overline{N} = 15$.

Example 1. Consider the DO time fractional problem

$$\int_0^1 \varpi(\mu)\,{}_0^C D_t^{\mu}\upsilon(x,y,t)\,d\mu = \frac{1}{4}\Delta\upsilon(x,y,t) + F(x,y,t),$$

with

$$F(x,y,t) = 10^5x^2(1-x)^2y^2(1-y)^2\left[\Gamma\left(\tfrac{5}{2}\right)x^2(1-x)^2y^2(1-y)^2\int_0^1\varpi(\mu)\frac{t^{\frac{3}{2}-\mu}}{\Gamma\left(\frac{5}{2}-\mu\right)}d\mu - t^{\frac{3}{2}}\left[y^2(1-y)^2(14x^2-14x+3)+x^2(1-x)^2(14y^2-14y+3)\right]\right],$$

where the exact solution is $\upsilon(x,y,t) = 10^5\,t^{\frac{3}{2}}x^4(1-x)^4y^4(1-y)^4$. Other required information can be derived from the expressed exact solution. The results achieved by our hybrid approach with $\bar{n} = 5, \beta = 0.9$ and different values of $\varpi(\mu), \bar{m}_1$and $\bar{m}_2$are presented in Table 1. The approximation solutions and the absolute error functions with $\bar{m}_1 = \bar{m}_2 = 9, \bar{n} = 5, \varpi(\mu) = \Gamma\left(\frac{3}{2}-\mu\right)$and $\beta = 0.9$are shown in Fig. 1 (right and left, respectively). According to the reported results, it can be concluded that in the suggested hybrid scheme, by increasing the number of the 2D CCFs, the accuracy and convergence order of the problem improve. Note that the numerical integration introduced in Section 5 is used to compute the integral appeared in the right side function. This work also will use for the next examples.

Table 1 Errors achieved with $\bar{n} = 5, \beta = 0.9$, several values of $(\bar{m}_1, \bar{m}_2)$ and two values of $\varpi(\mu)$ in Example 1.

	$\varpi(\mu) = \Gamma\left(\frac{3}{2}-\mu\right)$				$\varpi(\mu) = \Gamma\left(\frac{5}{2}-\mu\right)$			
$(\bar{m}_1, \bar{m}_2)$	L_∞	L_2	RMS	$\mathscr{CO}$	L_∞	L_2	RMS	$\mathscr{CO}$
$(4,4)$	6.4647×10^{-5}	4.7542×10^{-5}	1.1885×10^{-5}	-	6.3753×10^{-5}	4.6918×10^{-5}	1.1729×10^{-5}	-
$(5,5)$	2.2481×10^{-5}	1.7938×10^{-5}	3.5876×10^{-6}	4.7336	2.2311×10^{-5}	1.7724×10^{-5}	3.5449×10^{-6}	4.7052
$(6,6)$	9.9598×10^{-6}	6.8224×10^{-6}	1.1371×10^{-6}	4.4653	9.1524×10^{-6}	6.3497×10^{-6}	1.0583×10^{-6}	4.8873
$(7,7)$	4.2599×10^{-6}	3.4088×10^{-6}	4.8697×10^{-7}	5.5096	5.4363×10^{-6}	4.2330×10^{-6}	6.0472×10^{-7}	3.3793
$(8,8)$	1.9595×10^{-6}	1.5636×10^{-6}	1.9545×10^{-7}	5.8155	2.8725×10^{-6}	2.4086×10^{-6}	3.0108×10^{-7}	4.7773
$(9,9)$	6.2201×10^{-7}	4.7183×10^{-7}	5.2425×10^{-8}	9.7424	1.7832×10^{-6}	1.3541×10^{-6}	1.5046×10^{-7}	4.0479

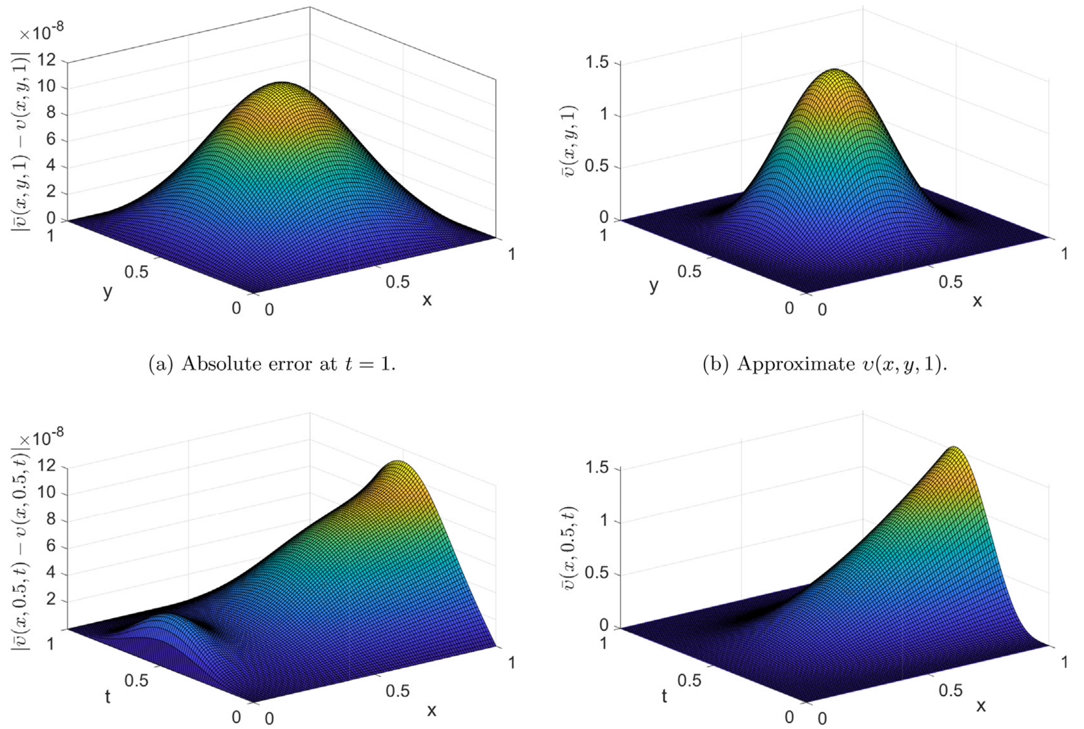

(a) Absolute error at $t=1$.

(b) Approximate $\upsilon(x,y,1)$.

(c) Absolute error at $y=0.5$.

(d) Approximate $\upsilon(x,0.5,t)$.

Fig. 1 Graphs of the results achieved for Example 1 with $(\bar{m}_1,\bar{m}_2)=(9,9),\bar{n}=5$, $\varpi(\mu)=\Gamma\left(\frac{3}{2}-\mu\right)$and $\beta=0.9$.

Example 2. Consider the DO time fractional problem

$$\int_0^1 \varpi(\mu)\,{}_0^C D_t^{\mu}\upsilon(x,y,t)\,d\mu=\Delta\upsilon(x,y,t)+F(x,y,t),$$

with

$$F(x,y,t)=10^3\,(1-x)^4(1-y)^4\left[\Gamma\left(\tfrac{7}{2}\right)(1-x)^2(1-y)^2\sin(x)\sin(y)\int_0^1\varpi(\mu)\frac{t^{\frac{5}{2}-\mu}}{\Gamma\left(\frac{7}{2}-\mu\right)}\,d\mu\right.$$
$$-t^{\frac{5}{2}}\Big[(1-y)^2\sin(y)((29+12x-x^2)\sin(x)-12(1-x)\cos(x))$$
$$\left.+(1-x)^2\sin(x)((29+12y-y^2)\sin(y)-12(1-y)\cos(y))\Big]\right],$$

where its analytic solution is $\upsilon(x,y,t)=10^3\,t^{\frac{5}{2}}(1-x)^6(1-y)^6\sin(x)\sin(y)$. The results achieved by our hybrid method with $\bar{n}=6,\beta=0.8$ for different values of $\varpi(\mu),\bar{m}_1$and $\bar{m}_2$are listed in Table 2. The approximation solutions and the absolute error functions with $\bar{m}_1=\bar{m}_2=9,\bar{n}=6,\varpi(\mu)=\Gamma\left(\frac{3}{2}-\mu\right)$ and $\beta=0.8$ are shown in Fig. 2 (right and left, respectively). According to the reported results, it can be realized that in the suggested hybrid scheme, by increasing the basis functions, the accuracy and convergence order of the outcomes ameliorates.

Example 3. Consider the DO time fractional problem

$$\int_0^1 \varpi(\mu)\,{}_0^C D_t^{\mu}\upsilon(x,y,t)\,d\mu=\frac{1}{2}\Delta\upsilon(x,y,t)+F(x,y,t),$$

with

Table 2 Errors achieved with $\bar{n}=6,\beta=0.8$, several values of $(\bar{m}_1,\bar{m}_2)$ and two values of $\varpi(\mu)$ in Example 2.

	$\varpi(\mu)=\Gamma\left(\frac{3}{2}-\mu\right)$				$\varpi(\mu)=\Gamma\left(\frac{5}{2}-\mu\right)$			
$(\bar{m}_1,\bar{m}_2)$	L_∞	L_2	RMS	$\mathscr{CO}$	L_∞	L_2	RMS	$\mathscr{CO}$
$(4,4)$	1.1530×10^{-2}	8.7033×10^{-3}	2.1758×10^{-3}	-	1.1463×10^{-2}	8.6560×10^{-3}	2.1640×10^{-3}	-
$(5,5)$	4.1440×10^{-3}	2.6286×10^{-3}	5.2573×10^{-4}	4.5580	4.0835×10^{-3}	2.5830×10^{-3}	5.1660×10^{-4}	4.6256
$(6,6)$	8.0423×10^{-4}	4.9217×10^{-4}	8.2028×10^{-5}	8.9925	7.5125×10^{-4}	4.5603×10^{-4}	7.6005×10^{-5}	9.2856
$(7,7)$	4.4451×10^{-5}	3.1078×10^{-5}	4.4397×10^{-6}	18.7836	9.4228×10^{-5}	6.5182×10^{-5}	9.3117×10^{-6}	13.4675
$(8,8)$	1.1143×10^{-5}	7.6893×10^{-6}	9.6116×10^{-7}	10.3614	9.0137×10^{-5}	6.7652×10^{-5}	8.4565×10^{-6}	0.3324
$(9,9)$	7.0021×10^{-6}	5.2828×10^{-6}	5.8697×10^{-7}	3.9946	8.5622×10^{-5}	6.5155×10^{-5}	7.2395×10^{-6}	0.4363

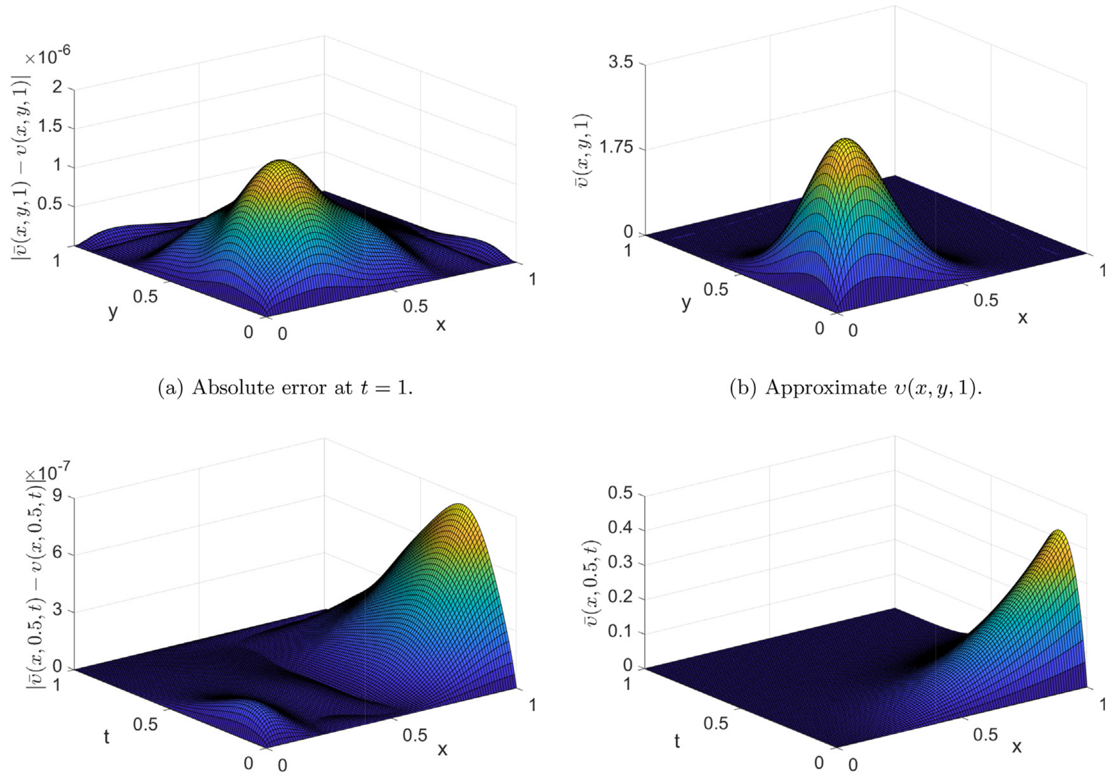

(a) Absolute error at $t = 1$.

(b) Approximate $\upsilon(x, y, 1)$.

(c) Absolute error at $y = 0.5$.

(d) Approximate $\upsilon(x, 0.5, t)$.

Fig. 2 Graphs of the results achieved for Example 2 with $(\bar{m}_1, \bar{m}_2) = (9, 9), \bar{n} = 6$, $\varpi(\mu) = \Gamma\left(\frac{3}{2} - \mu\right)$and $\beta = 0.8$.

Table 3 Errors achieved with $\bar{n} = 4, \beta = 0.7$, several values $(\bar{m}_1, \bar{m}_2)$ and two values of $\varpi(\mu)$ in Example 3.

	$\varpi(\mu) = \Gamma\left(\frac{3}{2} - \mu\right)$				$\varpi(\mu) = \Gamma\left(\frac{5}{2} - \mu\right)$			
$(\bar{m}_1, \bar{m}_2)$	L_∞	L_2	RMS	$\mathscr{CO}$	L_∞	L_2	RMS	$\mathscr{CO}$
$(3, 3)$	5.4329×10^{-6}	4.5342×10^{-6}	1.5114×10^{-6}	-	5.4609×10^{-6}	4.5568×10^{-6}	1.5189×10^{-6}	-
$(4, 4)$	1.4068×10^{-6}	1.0308×10^{-6}	2.5769×10^{-7}	4.6967	1.4017×10^{-6}	1.0268×10^{-6}	2.5669×10^{-7}	4.7272
$(5, 5)$	5.7811×10^{-7}	4.2913×10^{-7}	8.5825×10^{-8}	3.9854	5.8507×10^{-7}	4.3443×10^{-7}	8.6887×10^{-8}	3.9155
$(6, 6)$	2.5270×10^{-7}	1.7458×10^{-7}	2.9096×10^{-8}	4.5390	2.4564×10^{-7}	1.7018×10^{-7}	2.8364×10^{-8}	4.7601
$(7, 7)$	1.3679×10^{-7}	9.4847×10^{-8}	1.3550×10^{-8}	3.9815	1.4547×10^{-7}	1.0094×10^{-7}	1.4419×10^{-8}	3.3986
$(8, 8)$	5.4904×10^{-8}	3.4428×10^{-8}	4.3035×10^{-9}	6.8363	6.1910×10^{-8}	3.8385×10^{-8}	4.7981×10^{-9}	6.3977

$$
\begin{aligned}
F(x,y,t) = 10^6 x^4(1-x)^4 y^4(1-y)^4 e^{x+y} \\
\times \Bigg[\Gamma\left(\tfrac{9}{2}\right) x^2(1-x)^2 y^2(1-y)^2 \int_0^1 \varpi(\mu) \frac{t^{\frac{7}{2}-\mu}}{\Gamma\left(\frac{9}{2}-\mu\right)}\, d\mu \\
- \frac{t^{\frac{7}{2}}}{2}\Big[y^2(1-y)^2(x^4+22x^3+97x^2-120x+30) \\
+ x^2(1-x)^2(y^4+22y^3+97y^2-120y+30) \Big] \Bigg],
\end{aligned}
$$

where the true solution is $\upsilon(x,y,t) = 10^6\, t^{\frac{7}{2}} x^6(1-x)^6 y^6 (1-y)^6 e^{x+y}$. The results achieved by the utilized hybrid method with $\bar{n} = 4, \beta = 0.7$, two values of $\varpi(\mu)$and several values of $\bar{m}_1$and $\bar{m}_2$are provided in Table 3. The approximation solutions and the absolute error functions with $\bar{m}_1 = \bar{m}_2 = 9, \bar{n} = 4$, $\varpi(\mu) = \Gamma\left(\frac{5}{2} - \mu\right)$and $\beta = 0.7$are shown in Fig. 3 (right and left, respectively). According to the reported results, it can be realized that in the suggested hybrid scheme, by increasing the basis functions, the accuracy and convergence order of the outcomes ameliorates.

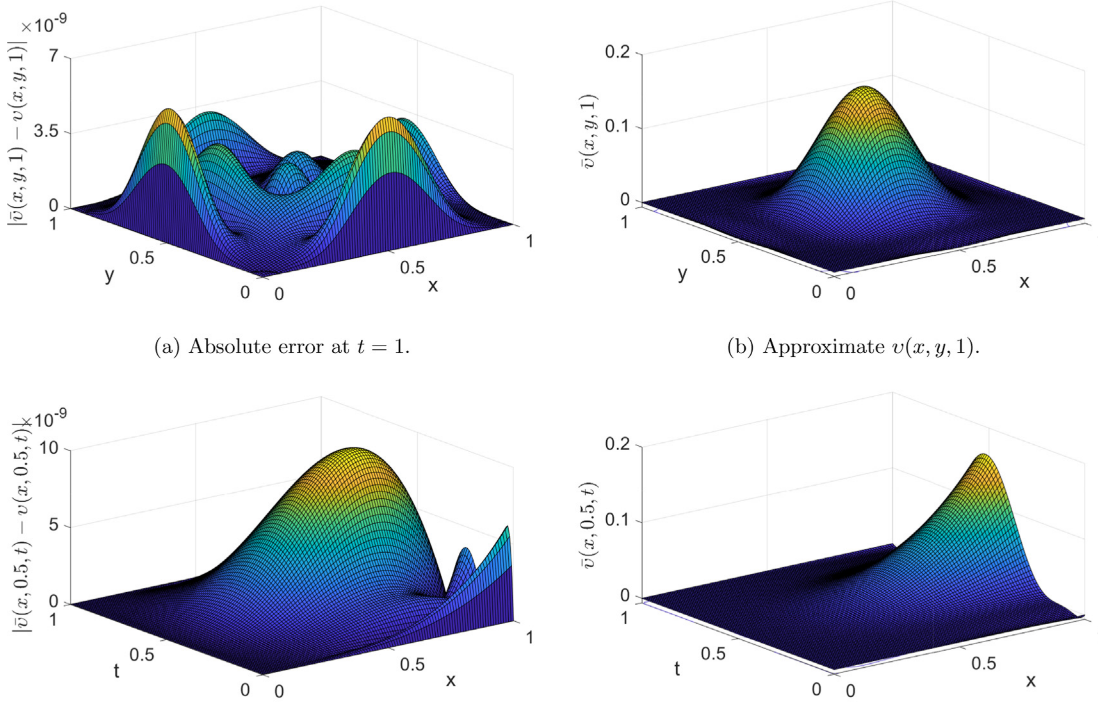

(a) Absolute error at $t = 1$.

(b) Approximate $v(x, y, 1)$.

(c) Absolute error at $y = 0.5$.

(d) Approximate $v(x, 0.5, t)$.

Fig. 3 Graphs of the results achieved for Example 3 with $(\bar{m}_1, \bar{m}_2) = (9, 9), \bar{n} = 4$, $\varpi(\mu) = \Gamma\left(\frac{5}{2} - \mu\right)$and $\beta = 0.7$.

7. Conclusion

This paper provided a hybrid approach to find a numerical solution for the DO fractional diffusion equation by employing the FEFs and 2D CCFs. The Caputo fractional derivative was applied to define the DO fractional derivative. To construct the expressed method, fractional derivative operational matrix for the FEFs and partial derivatives operational matrices for the 2D CCFs were achieved. Using operational matrices, the Gauss–Legendre quadrature formula and collocation approach, an algebraic system of equations was derived instead of the original problem that easily solved. The accuracy of the approach was tested by solving three examples, numerically. The yielded results confirm that the established hybrid approach is highly precise in solving such problems. As future research direction, the FEFs and 2D CCFs utilized in this paper can be developed for solving fractional versions of other applied problems, such as the extended Fisher–Kolmogorov and Klein–Gordon equations with this type of fractional derivative.

Declaration of Competing Interest

The authors declare that they have no known competing financial interests or personal relationships that could have appeared to influence the work reported in this paper.

References

[1] B. Ghanbari, On approximate solutions for a fractional prey–predator model involving the Atangana-Baleanu derivative, Adv. Diff. Eqs. (2020) 1–24.

[2] B. Ghanbari, On the modeling of the interaction between tumor growth and the immune system using some new fractional and fractional-fractal operators, Adv. Diff. Eqs. (2020) 1–32.

[3] B. Ghanbari, A fractional system of delay differential equation with nonsingular kernels in modeling hand-foot-mouth disease, Adv. Diff. Eqs. (2020) 1–20.

[4] B. Ghanbari, On novel nondifferentiable exact solutions to local fractional Gardner's equation using an effective technique, Math. Methods Appl. Sci. 44 (6) (2020) 4673–4685.

[5] B. Ghanbari, A new model for investigating the transmission of infectious diseases in a prey-predator system using a non-singular fractional derivative, Math. Methods Appl. Sci. (2021).

[6] B. Ghanbari, A. Atangana, Some new edge detecting techniques based on fractional derivatives with non-local and non-singular kernels, Adv. Diff. Eqs. (2020) 1–19.

[7] B. Ghanbari, On novel nondifferentiable exact solutions to local fractional Gardner's equation using an effective technique, Math. Methods Appl. Sci. 44 (6) (2021) 4673–4685.

[8] K. Kavitha, V. Vijayakumar, R. Udhayakumar, C. Ravichandran, Results on controllability of Hilfer fractional differential equations with infinite delay via measures of noncompactness, Asian J. Control 24 (3) (2022) 1406–1415.

[9] M.M. Raja, V. Vijayakumar, R. Udhayakumar, A new approach on approximate controllability of fractional evolution inclusions of order 1< r< 2with infinite delay, Chaos, Solitons and Fractals 141 (2020) 110343.

[10] M.M. Raja, V. Vijayakumar, R. Udhayakumar, Results on the existence and controllability of fractional integro-differential system of order 1< r< 2via measure of noncompactness, Chaos, Solitons and Fractals 139 (2020) 110299.

[11] V. Vijayakumar, R. Udhayakumar, A new exploration on existence of Sobolev-type Hilfer fractional neutral integro-differential equations with infinite delay, Numer. Methods Partial Differ. Eqs. 37 (1) (2021) 750–766.

[12] K. Kavitha, V. Vijayakumar, R. Udhayakumar, Results on controllability of Hilfer fractional neutral differential equations with infinite delay via measures of noncompactness, Chaos, Solitons and Fractals 139 (2020) 110035.
[13] O. Bavi, M. Hosseininia, M.H. Heydari, N. Bavi, SARS-CoV-2 rate of spread in and across tissue, groundwater and soil: A meshless algorithm for the fractional diffusion equation, Eng. Anal. Bound. Elem. 138 (2022) 108–117.
[14] S. Sabermahani, Y. Ordokhani, P. Rahimkhani, Application of two-dimensional Fibonacci wavelets in fractional partial differential equations arising in the financial market, Int. J. Appl. Comput. Math. 8 (3) (2022) 1–20.
[15] H. Azin, F. Mohammadi, J.A. Machado, A piecewise spectral-collocation method for solving fractional Riccati differential equation in large domains, Comput. Appl. Math. 38 (3) (2019) 1–13.
[16] F. Nourian, M. Lakestani, S. Sabermahani, Y. Ordokhani, Touchard wavelet technique for solving time-fractional Black-Scholes model, Comput. Appl. Math. 41 (4) (2022) 1–19.
[17] B. Yuttanan, M. Razzaghi, Thieu N. Vo, A numerical method based on fractional-order generalized Taylor wavelets for solving distributed-order fractional partial differential equations, Appl. Numer. Math. 160 (2021) 349–367.
[18] T.M. Atanackovic, S. Pilipovic, D. Zorica, Distributed-order fractional wave equation on a finite domain. stress relaxation in a rod, Int. J. Eng. Sci. 49 (2) (2011) 175–190.
[19] T.M. Atanackovic, A generalized model for the uniaxial isothermal deformation of a viscoelastic body, Acta Mech. 159 (1) (2002) 77–86.
[20] T.M. Atanackovic, M. Budincevic, S. Pilipovic, On a fractional distributed-order oscillator, J. Phys. A: Math. Gen. 38 (30) (2005) 6703.
[21] M.A. Zaky, J.A. Tenreiro Machado, On the formulation and numerical simulation of distributed-order fractional optimal control problems, Commun. Nonlinear Sci. Numer. Simul. 52 (2017) 177–189.
[22] M. Pourbabaee, A. Saadatmandi, A new operational matrix based on Müntz-Legendre polynomials for solving distributed order fractional differential equations, Math. Comput. Simul. 194 (2022) 210–235.
[23] P. Rahimkhani, Y. Ordokhani, Solving of partial differential equations with distributed order in time using fractional-order Bernoulli-Legendre functions, Comput. Methods Diff. Eqs. 9 (3) (2021) 799–817.
[24] L. Li, F. Liu, L. Feng, I. Turner, A Galerkin finite element method for the modified distributed-order anomalous sub-diffusion equation, J. Comput. Appl. Math. 368 (2020) 112589.
[25] Y. Xu, Y. Zhang, J. Zhao, Error analysis of the Legendre-Gauss collocation methods for the nonlinear distributed-order fractional differential equation, Appl. Numer. Math. 142 (2019) 122–138.
[26] B. Yuttanan, M. Razzaghi, Legendre wavelets approach for numerical solutions of distributed order fractional differential equations, Appl. Math. Model. 70 (2019) 350–364.
[27] M.A. Zaky, A.S. Hendy, J.E. Macías-Díaz, Semi-implicit Galerkin-Legendre spectral schemes for nonlinear time-space fractional diffusion–reaction equations with smooth and nonsmooth solutions, J. Sci. Comput. 82 (1) (2020) 1–27.
[28] R.L. Magin, Fractional calculus models of complex dynamics in biological tissues, Comput. Math. Appl. 59 (5) (2010) 1586–1593.
[29] Y.A. Rossikhin and M.V. Shitikova. Applications of fractional calculus to dynamic problems of linear and nonlinear hereditary mechanics of solids. 1997.
[30] H. Patel, T. Patel, D. Pandit, An efficient technique for solving fractional-order diffusion equations arising in oil pollution, J. Ocean Eng. Sci. (2022).
[31] C. Xie, S. Fang, Efficient numerical methods for Riesz space-fractional diffusion equations with fractional Neumann boundary conditions, Appl. Numer. Math. 176 (2022) 1–18.
[32] C. Zhu, B. Zhang, H. Fu, J. Liu, Efficient second-order ADI difference schemes for three-dimensional Riesz space-fractional diffusion equations, Computers & Mathematics with Applications 98 (2021) 24–39.
[33] J.L. Zhang, Z.W. Fang, H.W. Sun, Exponential-sum-approximation technique for variable-order time-fractional diffusion equations, Journal of Applied Mathematics and Computing 68 (1) (2022) 323–347.
[34] M. Hosseininia, M.H. Heydari, Z. Avazzadeh, A hybrid approach established upon the Müntz-Legender functions and 2D Müntz-legender wavelets for fractional Sobolev equation, Mathematical Methods in the Applied Sciences (2022).
[35] A. Rayal, S.R. Verma, Numerical analysis of pantograph differential equation of the stretched type associated with fractal-fractional derivatives via fractional order Legendre wavelets, Chaos, Solitons and Fractals 139 (2020) 110076.
[36] S.K. Sharma, D. Kumar, A numerical study of new fractional model for convective straight fin using fractional-order Legendre functions, Chaos, Solitons and Fractals 141 (2020) 110282.
[37] P. Rahimkhani, Y. Ordokhani, Approximate solution of nonlinear fractional integro-differential equations using fractional alternative Legendre functions, J. Comput. Appl. Math. 365 (2020) 112365.
[38] S. Rezabeyk, S. Abbasbandy, E. Shivanian, Solving fractional-order delay integro-differential equations using operational matrix based on fractional-order Euler polynomials, Mathematical Sciences 14 (2) (2020) 97–107.
[39] H. Dehestani, Y. Ordokhani, A modified numerical algorithm based on fractional Euler functions for solving time-fractional partial differential equations, International Journal of Computer Mathematics 98 (10) (2021) 2078–2096.
[40] Y. Wang, L. Zhu, Z. Wang, Fractional-order Euler functions for solving fractional integro-differential equations with weakly singular kernel, Advances in Difference Equations (2018) 1–13.
[41] K. Krishnarajulu, R.B. Sevugan, G.V. Sivaramakrishnan, A new approach to space fractional differential equations based on fractional order Euler polynomials, Publications de l'Institut Mathematique 104 (118) (2018) 157–168.
[42] M. Hosseininia, M.H. Heydari, M.R. Hooshmandasl, F.M. Maalek Ghaini, Z. Avazzadeh, A numerical method based on the Chebyshev cardinal functions for variable-order fractional version of the fourth-order 2D Kuramoto-Sivashinsky equation, Mathematical Methods in the Applied Sciences 44 (2) (2021) 1831–1842.
[43] M.H. Heydari, A. Atangana, Z. Avazzadeh, Y. Yang, Numerical treatment of the strongly coupled nonlinear fractal-fractional Schrödinger equations through the shifted Chebyshev cardinal functions, Alexandria Eng. J. 59 (4) (2020) 2037–2052.
[44] Y. Luchko, Boundary value problems for the generalized time-fractional diffusion equation of distributed order, Fract. Calc. Appl. Anal 12 (4) (2009) 409–422.
[45] M. Dehghan, M. Lakestani, The use of Chebyshev cardinal functions for solution of the second-order one-dimensional telegraph equation, Numer. Methods Partial Diff. Eqs. 25 (4) (2009) 931–938.
[46] M.H. Heydari, Chebyshev cardinal functions for a new class of nonlinear optimal control problems generated by Atangana-Baleanu-Caputo variable-order fractional derivative, Chaos, Solitons and Fractals 130 (2020) 109401.
[47] M. Lakestani, M. Dehghan, The use of Chebyshev cardinal functions for the solution of a partial differential equation with an unknown time-dependent coefficient subject to an extra measurement, J. Comput. Appl. Math. 235 (3) (2010) 669–678.

[48] A. Afarideh, F.D. Saei, M. Lakestani, B.N. Saray, Pseudospectral method for solving fractional Sturm-Liouville problem using Chebyshev cardinal functions, Phys. Scr. 96 (12) (2021) 125267.

[49] I. Podlubny, Fractional differential equations: an introduction to fractional derivatives, fractional differential equations, to methods of their solution and some of their applications, Elsevier, 1998.

[50] M. Razzaghi, Y. Ordokhani, N. Haddadi, Direct method for variational problems by hybrid of block-pulse and Bernoulli polynomials, 2012.

[51] A. Quarteroni, T. Zang, C. Canuto, M. Hussaini, Spectral methods in fluid dynamics, Springer-Verlage, Berlin, 1998.